Supporting Information

for

Effect of nonmagnetic ion deficiency on magnetic structure: Density functional study of $Sr_2MnO_2Cu_{2-x}Te_2$, $Sr_2MO_2Cu_2Te_2$ (M = Co, Mn), and the oxide-hydrides Sr_2VO_3H, $Sr_3V_2O_5H_2$ and $SrVO_2H$

Hyun-Joo Koo[a,*] and Myung-Hwan Whangbo[b,c,d,*]

[a] Department of Chemistry and Research institute for Basic Sciences, Kyung Hee University, Seoul, 02447, Republic of Korea

[b] Department of Chemistry, North Carolina State University, Raleigh, NC 27695-8204, USA

[c] State Key Laboratory of Structural Chemistry, Fujian Institute of Research on the Structure of Matter (FJIRSM), Chinese Academy of Sciences (CAS), Fuzhou, China, 350002

[d] State Key Laboratory of Crystal Materials, Shandong University, Jinan, China, 250100

[1] Evaluation of the magnetic anisotropies by DFT+U+SOC calculations

To evaluate the magnetic anisotropy of a V^{3+} ion in the oxide-hydrides, we substitute nonmagnetic Ga^{3+} ions for all V^{3+} ions except for one in a unit cell so as to isolate one VO_4H_2 embedded in the oxide-hydrides and then carry out DFT+U+SOC calculations for the cases of ||z and ⊥z spin orientations of the V^{3+} ion. A similar method was used to evaluate the magnetic anisotropy of the M^{2+} ion of $Sr_2MO_2Cu_2Te_2$ (M = Co, Mn) by replacing all M^{2+} ions except for one with nonmagnetic Zn^{2+} ions to isolate one MO_4Te_2 octahedron embedded in the solid. In each MnO_2Te_2 layer of $Sr_2MnO_2Cu_{1.5}Te_2$ with 10 % breathing-mode Mn-O bond contraction, each supercell has two Mn^{2+} and two Mn^{3+} ions. To isolate one MnO_4Te_2 octahedron containing a Mn^{2+} ion per supercell, we replace the remaining Mn^{2+} ion with Zn^{2+} and two Mn^{3+} ions with Ga^{3+}. Similarly, to isolate one MnO_4Te_2 octahedron containing a Mn^{3+} ion per supercell, we replace the remaining Mn^{3+} ion with Ga^{3+} and two Mn^{2+} ions with Zn^{2+}.

[2] Supplementary tables

Table S1. The geometrical parameters associated with the exchange paths, where the distance are in Angstrom and the angles are in degrees.

(a) Sr_2VO_3H

	V…V	V-L (L = H, O)	∠V-L-V (L = H, O)
J_1	3.6601	1.8300	180.0
J_2	3.8853	1.9426	180.0

(b) $Sr_3V_2O_5H_2$

	V…V	V-L (L = H, O)	∠V-L-V (L = H, O)
J_1	3.6584	1.8307	175.4
J_2	3.9114	1.9559	178.3
$J_{2'}$	3.8706	1.9353	180.0

(c) $SrVO_2H$

	V…V	V-L (L = H, O)	∠V-L-V (L = H, O)
J_1	3.6671	1.8335	180.0
J_2	3.9331	1.9665	180.0

(d) CoO_2Te_2 layers of $Sr_2CoO_2Cu_2Te_2$

	Co…Co	Co-O	∠Co-O-Co
J_1	4.1523	2.0761	180.0
	Co…Co	O…O	∠Co-O…O
J_2	5.8722	2.9361	135.0

(e) MnO_2Te_2 layers of $Sr_2MnO_2Cu_2Te_2$

	Mn…Mn	Mn-O	∠Mn-O-Mn
J_1	4.1700	2.0850	180.0
	Mn…Mn	O…O	∠Mn-O…O
J_2	5.8972	2.9486	135.0

Table S2. Expressions of the ordered spin states in terms of the spin exchanges

(a) Sr_2VO_3H

	J_1S^2	J_2S^2
E_{FM}	+8	+8
E_{AF1}	-8	-8
E_{AF2}	-8	+8

(b) $Sr_3V_2O_5H_2$

	J_1S^2	J_2S^2	J'_2S^2
E_{FM}	+16	+16	+8
E_{AF1}	-16	-16	+8
E_{AF2}	-16	+16	+8
E_{AF3}	+16	+16	-8

(c) $SrVO_2H$

	J_1S^2	J_2S^2
E_{FM}	+8	+16
E_{AF1}	-8	+16
E_{AF2}	-8	-16

(d) MoO_2Te_2 layers of $Sr_2MO_2Cu_2Te_2$ (M = Co, Mn) and $Sr_2MnO_2Cu_{1.5}Te_2$

	J_1S^2	J_2S^2
E_{FM}	+8	+8

E_{AF1}	-8	+8
E_{AF2}	0	-8

Table S3. Relative energies (meV per formula unit) of the ordered spin states calculated by DFT+U calculations

(a) Sr_2VO_3H

	U^{eff} = 3 eV	U^{eff} = 4 eV
E_{FM}	101	83
E_{AF1}	0	0
E_{AF2}	87	72

(b) $Sr_3V_2O_5H_2$

	U^{eff} = 3 eV	U^{eff} = 4 eV
E_{FM}	185	153
E_{AF1}	0	0
E_{AF2}	165	136
E_{AF3}	91	75

(c) $SrVO_2H$

	U^{eff} = 3 eV	U^{eff} = 4 eV
E_{FM}	162	134
E_{AF1}	155	128
E_{AF2}	0	0

(d) MO_2Te_2 layers of $Sr_2MO_2Cu_2Te_2$ (M = Co, Mn) and $Sr_2MnO_2Cu_{1.5}Te_2$

	M = Co	M = Mn

	U^{eff} = 3 eV	U^{eff} = 4 eV	U^{eff} = 5 eV	U^{eff} = 3 eV	U^{eff} = 4 eV	U^{eff} = 5 eV
E_{FM}	96	76	60	39 (0)[a]	32 (0)[a]	24 (0)[a]
E_{AF1}	0	0	0	0 (202)	0 (203)	0 (195)
E_{AF2}	40	32	25	17 (83)	12 (91)	8 (97)

[a] The numbers in the parentheses refer to $Sr_2MnCu_{1.5}Te_2O_2$, and those outside the parentheses to $Sr_2MnCu_{1.5}Te_2O_2$.

[3] Supplementary figures

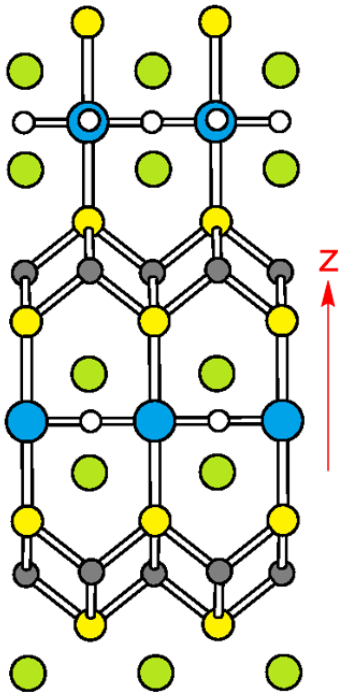

Figure S1. Projection view of the crystal structure of stoichiometric $Sr_2MO_2Cu_2Te_2$ (M = Co, Mn) along the a-direction, where Sr = green sphere, M = blue sphere, O = white sphere, Te = yellow sphere, and Cu = grey sphere.

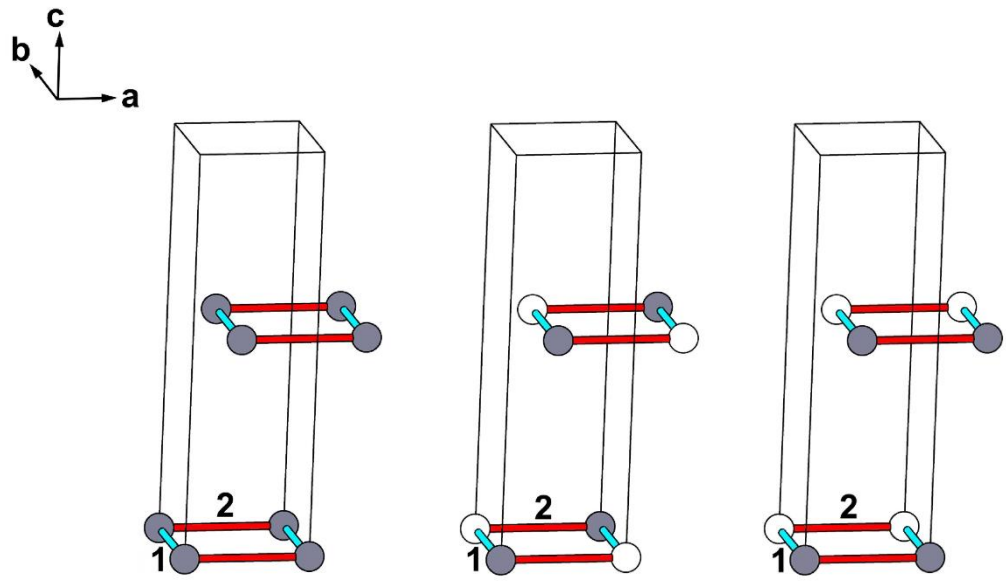

(a) FM (b) AF1 (c) AF2

Figure S2. Three ordered spin states used to carry out the energy mapping analysis for Sr_2VO_3H, where the filled and empty spheres represent the up-spin and down-spin V^{3+} sites, respectively.

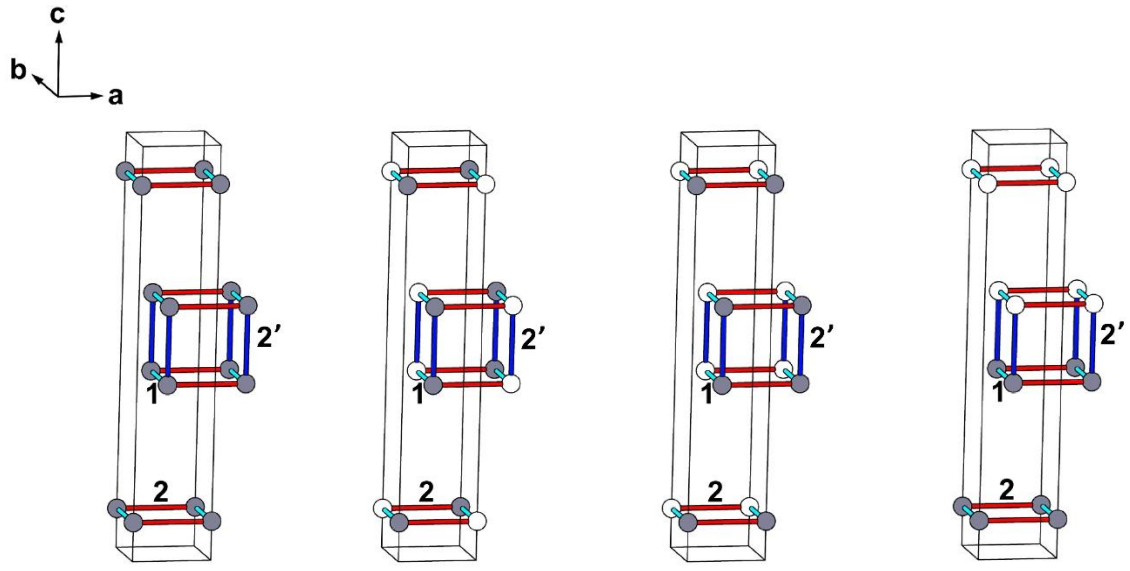

(a) FM (b) AF1 (c) AF2 (d) AF3

Figure S3. Four ordered spin states used to carry out the energy mapping analysis for $Sr_3V_2O_5H_2$, where the filled and empty spheres represent the up-spin and down-spin V^{3+} sites, respectively.

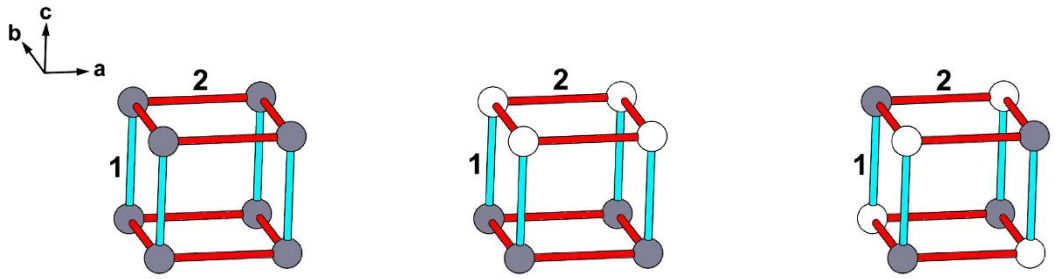

(a) FM (b) AF1 (c) AF2

Figure S4. Three ordered spin states used to carry out the energy mapping analysis for $SrVO_2H$, where the filled and empty spheres represent the up-spin and down-spin V^{3+} sites, respectively.

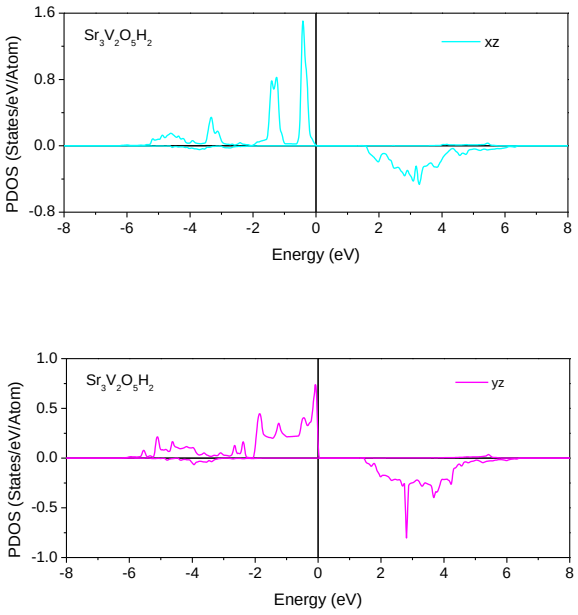

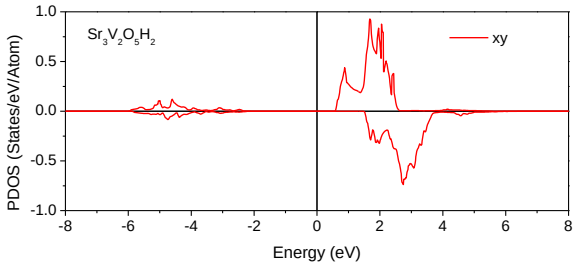

Figure S5. PDOS plots calculated for the d_{xz}, d_{yz}, d_{xy} states of $Sr_3V_2O_5H_2$ obtained by DFT+U calculations with U^{eff} = 3 eV.

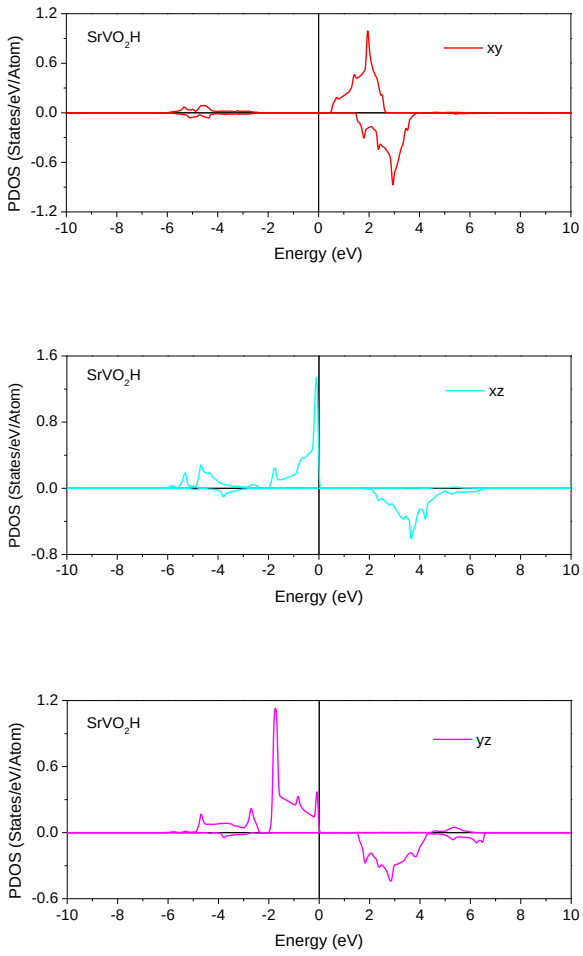

Figure S6. PDOS plots calculated for the d_{xz}, d_{yz}, d_{xy} states of $SrVO_2H$ obtained by DFT+U calculations with U^{eff} = 3 eV.

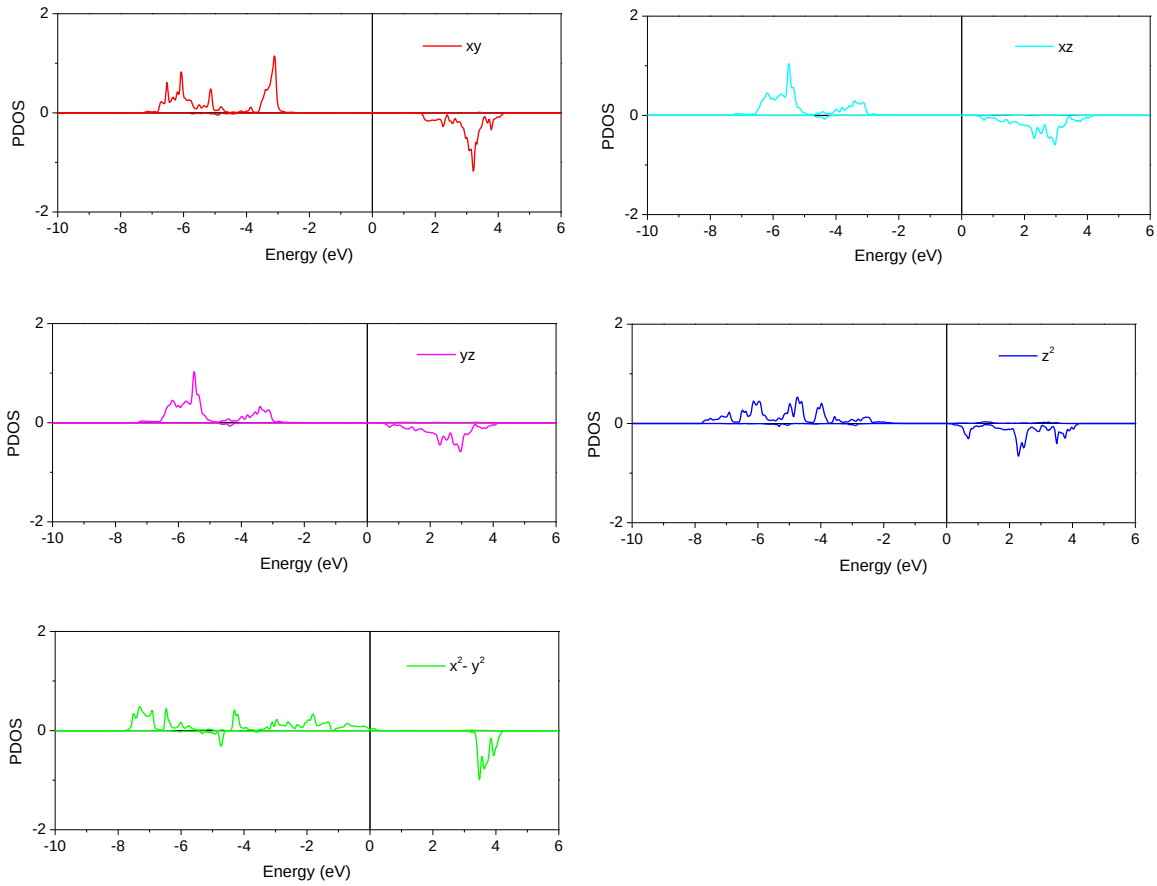

Figure S7. PDOS plots calculated for the d-states of $Sr_2MnCu_2Te_2O_2$ by DFT+U calculations using U^{eff} = 4 eV.